Catalysis Today 137 (2008) 125–131

Contents lists available at ScienceDirect

Catalysis Today

journal homepage: www.elsevier.com/locate/cattod

Cerium(IV)oxide modification by inclusion of a hetero-atom: A strategy for producing efficient and robust nano-catalysts for methanol carboxylation

Michele Aresta [a,*], Angela Dibenedetto [a], Carlo Pastore [a], Corrado Cuocci [b], Brunella Aresta [b], Stefania Cometa [c], Elvira De Giglio [c]

[a] Department of Chemistry and CIRCC, University of Bari, Campus Universitario, 70126 Bari, Italy
[b] Istituto di Cristallografia, CNR, via Amendola 122, 70126 Bari, Italy
[c] Department of Chemistry, University of Bari, Via Amendola 173, 70126 Bari, Italy

ARTICLE INFO

Keywords:
Cerium(IV) oxide
Al-loaded catalysts
Fe-loaded catalysts
Nano-catalysts
Methanol carboxylation
Catalyst stability

ABSTRACT

Cerium(IV) oxide has been reported to catalyse the direct carboxylation of methanol to dimethylcarbonate, DMC. Nevertheless, the life of commercially available catalysts is quite short as after the first cycle the activity decreases and after a few cycles goes to zero. Noteworthy, no reports are in the literature about the stability of catalysts and their life. We have investigated the behaviour of catalysts and their de-activation using either surface techniques, such as XPS, or structural techniques, such as XRD. The reduction of Ce(IV) to Ce(III) and surface modification seem to be responsible for de-activation of the oxide. The results of a detailed study correlating the size and structure of particles to the activity of the catalysts are reported in this paper. In particular, pure commercial CeO_2 is compared, using High Throughput Experiments (HTE), with CeO_2 synthesised in our laboratory and with the latter loaded with Al or Fe at various concentrations. The hetero-metals have a different effect on the stabilization of the Ce-catalyst and on its activity. Al-loaded CeO_2 affords the most interesting results in terms of lifetime and activity. Therefore, the correlation of the structural properties of CeO_2 loaded with Al at a concentration variable between 3 and 40% to the activity in catalysis is discussed in detail. XPS and XRD data have been used for the characterization of the catalyst before and after a catalytic run. Pure synthesised CeO_2 and CeO_2 loaded with Al are able to maintain their activity for several cycles (apparent TON of several tens) or three days of operation without any treatment after recovery, with a much better performance than the commercial catalysts that, conversely, loose their activity after a few cycles. The size of the particles determines the activity of the catalyst and we show that particles having a size 15–60 nm are the most active, while particles sized micrometers are much less active.

1. Introduction

The direct carboxylation of methanol to dimethylcarbonate (DMC) attracts much attention worldwide because DMC finds a large utilization in several industrial applications. In fact, DMC is used in the chemical industry as monomer for polymers, [1] in transesterification reactions for the production of other carbonates such as diphenylcarbonate [2] and others, as alkylating or carboxylating agent [3,4]. It is also used in the agrochemical [5] and pharmaceutical industry [6] for the production of chemicals or in product formulation. A new potential application of DMC is an additive to gasoline that would expand its market by over one order of magnitude. Such potential use requires the implementation of new synthetic methodologies because the technologies on stream, either that based on the use of phosgene or the newest one based on the oxidative carbonylation of methanol [7,8], suffer from several drawbacks that prevent the expansion of the production to the desired amount.

More recently, the direct carboxylation of methanol (Eq. (1)), a reaction that responds to the principles of the sustainable chemical industry, has been investigated by several research groups worldwide.

$$2CH_3OH + CO_2 \rightleftharpoons (CH_3O)_2CO + H_2O \quad (1)$$

Both homogeneous and heterogeneous catalysts have been used so far. Among the former, Sn [9] and Nb [10] show interesting properties. Nevertheless, their exploitation is limited by the conversion of tin catalysts into oligomers during catalysis, that reduces their activity; while Nb(V)-alkoxo species maintain their activity until they are in an almost anhydrous reaction medium. Unfortunately, the formation of water in reaction (1) causes the de-

* Corresponding author. Tel.: +39 080 544 20 84; fax: +39 080 544 36 06.
E-mail address: m.aresta@chimica.uniba.it (M. Aresta).

0920-5861/$ – see front matter © 2008 Elsevier B.V. All rights reserved.
doi:10.1016/j.cattod.2008.04.043

activation of the catalyst or forces the adoption of energy consuming methodologies, such as the recovery of the catalyst at the end of each reaction cycle and its re-use in anhydrous methanol. The use of water-traps has also been attempted. Organic water traps such as aldols, [11] ketals, [12] ortoformates, [13] although rise the problem of separation from the reaction mixture, are more efficient than inorganic systems such as zeolites as the latter at the working temperature (470 K) may act as protonating agents of DMC, reversing the reaction. Cooling of the reaction mixture to room temperature, dewatering and reheating has been [14] adopted as a strategy for using zeolites as water traps. DCC [15] has shown a very interesting behaviour as it alone is able to promote the formation of DMC under very mild conditions (310 K and 0.2 MPa) with excellent yield (>90%) and selectivity (>98%). Unfortunately, 1 mol of DCC is converted into the relevant urea (Eq. (2)) per mol of DMC produced: this makes that unless the urea is quantitatively converted back to DCC such synthetic methodology is not economically convenient for exploitation.

$$CyN{=}C{=}NCy + 2CH_3OH + CO_2 \rightarrow DMC + CyHNC(O)NHCy \quad (2)$$

Heterogeneous catalysts such as CeO_2, [16] ZrO_2 [17] or TiO_2 [18] have also been used but they in general suffer of a serious drawback represented by their de-activation: after the first cycle their activity decreases to a marginal conversion of methanol.

In this work, we have investigated the reasons of the degradation of commercial CeO_2 and developed a new synthetic methodology for CeO_2 tested in the carboxylation of methanol. We have also synthesized and tested in catalysis CeO_2 loaded with metals such as Al and Fe. The behaviour of CeO_2 loaded with 10% Al_2O_3 is described in detail. XRD and surface techniques such as BET and XPS have been used for the characterization of the catalysts before and after use in catalysis.

2. Experimental section

All solvents, starting reagents and the commercial metal oxides listed in Table 1 were RP Aldrich products. Methanol was dried, distilled [19] and stored under dinitrogen (the residual water was 20 ppm, as determined by the Karl-Fisher method, using a Metrohm 785 DMP Titrino apparatus). Carbon dioxide was from Rivoira IP (99.999% purity).

Nuclear magnetic resonance (NMR) experiments were carried out with a 400 MHz Varian INOVA apparatus (9.39 T) using the MAS technique with a basic frequency of 104.215 MHz for the aluminium nucleus. The samples were packed in a 5 mm diameter zirconia rotor and spinned at 5 kHz during the analysis. The 90° pulse duration was 4.5 μs with a subsequent relaxation time of 4 s. The number of transients changed with the aluminium content in order to obtain good spectra in terms of signal-to-noise ratio. All the chemical shifts were calculated taking as reference an aqueous solution of aluminium as $[Al(H_2O)_6]^{3+}$.

FTIR spectra were recorded with a Shimadzu Prestige 21 instrument.

X-ray Photoelectron Spectroscopy (XPS) spectra were obtained using a ThermoVG Thetaprobe spectrometer, equipped with a microspot monochromatised Al-Kα source and the gun of low-energy electrons for compensation of electrostatic charging of samples. The Al-Kα line (1486.6 eV) was used throughout this work and the base pressure of the instrument was 10^{-9} mbar. Survey scans (binding energy range 0–1200 eV, FAT mode, pass energy = 200 eV) and detailed spectra (FAT mode, pass energy = 50 eV) were recorded for each sample. Data analysis of the latter was performed using the Avantage software package, which consists of a non-linear least-squares fitting program. The values of binding energies BE (eV) were taken relatively to the binding energy of Cls-electrons of hydrocarbons on the sample surface (produced by adventitious carbon), which is accepted to be equal to 285.0 eV. Quantification was performed using peak areas; comparison between data from different elements was possible after correction (division) by empirically derived atomic sensitivity factors.

Table 1
Comparison of the activity of single metal- or bimetallic-oxides

Entry	Catalyst	Conversion (%)	mmol of DMC/ mmol of catalyst
1	$Al(OH)_3$	0.051	0.045
2	$Al(OH)_3$[a]	0.002	0.001
3	$CeSO_4$	0.048	0.095
4	Ce_2O_3	0	0
5	Al_2O_3 SiO_2	0	0
6	Al_2O_3 SiO_2[a]	0.001	0.002
7	La_2O_3	0	0
8	La_2O_3[a]	0.001	0.001
9	$KTiNbO_5$	0.001	0.001
10	CeO_2 sint 2 h calc.[b]	0.352	0.30
11	Al/Ce (3%) 2 h calc.	0.400	0.37
12	Al/Ce (3%) 3 h calc.[c]	0.425	0.40
13	Al/Ce (10%) 2 h calc.	0.243	0.20
14	Al/Ce (10%) 3 h calc.	0.423	0.34
15	Al/Ce (20%) 2 h calc.	0.207	0.15
16	Al/Ce (20%) 3 h calc.	0.325	0.25
17	Fe/Ce (1%)	0.101	0.09
18	Fe/Ce (3%)	0.314	0.27
19	Fe/Ce (7%)	0.448	0.38

The yield of DMC was estimated after 3 h of reaction between 4 mL of methanol, CO_2 (5.0 MPa) and 100 mg of catalyst, at 408 K. The "conversion" means the percent of alcohol converted into DMC (the latter was evaluated gas-chromatographically using toluene as internal standard). In the last column, the molar ratio of DMC to the total number of moles of the metal is reported.

[a] Commercial compounds calcinated for 2 h at 923 K on air.

[b] Oxide obtained via calcination for 2 h at 923 K on air of the synthesized mixed hydroxide.

[c] Oxide obtained via calcination for 3 h at 923 K on air of the synthesized mixed hydroxide.

X-rays diffraction spectra-XRD spectra were taken using a Bruker D8-DISCOVER diffractometer, in reflection geometry using a flat sample, with a X-Ray tube using the Cu-Kα line (λ-Kα1 = 1.54056 Å and λ-Kα2 = 1.54439 Å). The tests were done in a short period of time so that the same experimental conditions were preserved. The experimental parameters were: step-scan 0.03°, 2θ range from 25 to 135°, 20 s acquisition time.

XRD-spectra were compared with different diffraction patterns of cerium oxide present in PDF (powder diffraction file) data bank using DIFFRACplus EVA [20] for qualitative analysis to check out the chemical phase present in the powder. XRD-spectra data were processed using EXPO2006 [21] for structural analysis and FullProf/Topas [22,23] for structural refinement according to the Rietveld method [24]. The peak profiles were fitted with Pearson VII function to calculate the crystallite size and the full width at half maximum (FWHM).

GC–MS analyses were carried out with a gas chromatograph Shimadzu 17 A (capillary column: 30 m; MDN-5S; ∅ 0.25 mm, 0.25 μm film) coupled to a Shimadzu QP5050 A mass spectrometer. Quantitative determinations on the reaction solutions were performed using Hewlett Packard 6850 GC-FID (capillary column: 30 m; Carbowax; ∅ 0.25 mm, 0.25 μm film).

BET areas were determined with a Micromeritics Chemisorb 2750 equipment.

2.1. Synthesis of CeO_2

Two methodologies were used for the synthesis of the oxide, starting from either $Ce(NO_3)_3{\cdot}6H_2O$ (method A) or $(NH_4)_2Ce(NO_3)_6$ (method B).

Method A: 5.05 g of $Ce(NO_3)_3{\cdot}6H_2O$ was dissolved in H_2O (10 mL) and a solution 1:10 (v/v) of NH_4OH (20 mL) was added very slowly until pH 9 was reached. The precipitation of $Ce(OH)_3$ was observed. The suspension was centrifuged and the isolated solid calcinated in the air at 923 K for 3 h (yield = 84.6%). The BET area was determined to be 60–70 $m^2\ g^{-1}$.

Method B: $(NH_4)_2Ce(NO_3)_6$ (2.96 g) was dissolved in H_2O (10 mL) and a NH_4OH solution (25 mL) was added to reach a pH 9. The solid isolated by centrifugation was calcinated at 873–923 K for 3 h (yield = 92.5%). The BET area was 65–75 $m^2\ g^{-1}$.

XPS and XRD analyses (see the Section 3) were used to characterize the synthesized oxides: they did show that the samples were identical.

2.2. Synthesis of 3% Al/Ce mixed oxides

$Ce(NO_3)_3{\cdot}6H_2O$ (5.21 g) was dissolved in 10 mL of a $Al(NO_3)_3$ solution (1 mg of Al/mL). The system was stirred for 1 h and then 28 mL of NH_4OH solution 1:10 (v/v) were added in order to reach a pH value of 9. The precipitated solid was isolated by centrifugation and calcinated in the air at 873–923 K for 3 h to obtain Al/Ce mixed oxides (yield = 76%). ^{27}Al NMR MAS, XPS and XRD analyses were used to characterize the oxide as reported in the Section 3. The BET area was 80–90 $m^2\ g^{-1}$.

2.3. Synthesis of Al/Ce mixed oxides (10, 20 and 40%)

In order to synthesize the mixed oxides at 10% of aluminium, the starting load of aluminium was 10 mL of the standard solution mentioned above in which 1.47 g of $Ce(NO_3)_3{\cdot}6H_2O$ was dissolved, while for the mixed oxide at 20 and 40% of aluminium 20 and 40 mL of the standard solution was used, respectively, to dissolve 1.29 g of $Ce(NO_3)_3{\cdot}6H_2O$.17 and 25 mL of NH_4OH solution 1:10 (v/v) were used, respectively, to precipitate the two metals as the relevant hydroxides. The same procedure described for the synthesis of the mixed oxide at 3% was used in order to isolate the mixed oxides. Analogously, ^{27}Al NMR-MAS, XPS and XRD analyses were used to characterize the oxides synthesized (see the Section 3). The BET area was 70–80 $m^2\ g^{-1}$.

2.4. Synthesis of 1% Fe/Ce mixed oxides

2.5135 g of $Ce(NO_3)_3{\cdot}6H_2O$ was dissolved into 10 mL of a standard solution of iron (1 mg of Fe/mL) and oxides were co-precipitated with the addition of 20 mL of a NH_4OH solution (10%, v/v) as the relevant hydroxides. The solid obtained by centrifugation was calcined in air at a temperature of 923 K for 3 h with a final yield of 81.4% of the isolated oxide.

Fe elemental analysis: theoretical 1.0% vs an experimental content of 0.9%.

XPS analyses were used to characterize the oxide synthesized. The signals of cerium are the same reported in Fig. 4 for CeO_2, and the Fe binding energy signal is located at 717 eV.

2.5. Synthesis of Fe/Ce mixed oxides (3 and 7%)

The mixed oxides at higher concentration of iron (3 and 7%), were obtained following the same procedure described above using 0.6996 and 0.3104 g of $Ce(NO_3)_3{\cdot}6H_2O$, respectively, in 10 mL of a standard solution of iron (1 mg of Fe/mL). The relevant elemental analysis are 3.4% vs a theoretical value of 3.6% for the Fe–Ce $3\%_m$ oxide, but for the Fe–Ce $7\%_m$ oxide we find an experimental value of 7.7% vs a theoretical of 7.3%.

XPS analyses were used to characterize the final oxides. The signals of cerium are the same reported in Fig. 4 for CeO_2, and the Fe(III) binding energy signal is located at 717 eV.

Fig. 1. 4-parallel stainless steel autoclave.

2.6. Catalytic tests

The reaction of carboxylation of methanol was run using a 4-parallel stainless steel autoclave (Fig. 1) (the inner volume of each reactor was 10 mL). In each test 100 mg of oxide were used with 4 mL of methanol under 5.0 MPa of carbon dioxide and 10 μL of toluene as internal standard. The autoclave was heated at 408 K for 3 h. At the end of the cycle, the autoclave was cooled to room temperature and after the gas-chromatographic analysis of the organic phase, the oxides were recovered by filtration, dried under vacuum at room temperature and reused with new fresh dry methanol. After five cycles of reactivity, the oxide was analysed by XPS and XRD. The organic phase was analysed by GC and GC–MS.

3. Results and discussion

3.1. Characterization of CeO_2 before and after use in catalysis

Commercial CeO_2 was used in the carboxylation of methanol at 423 K under 5 MPa of CO_2. Anhydrous methanol was used in each catalytic run that was extended to the time necessary to reach the equilibrium concentration of DMC. Fig. 2 shows the trend of the formation of DMC with time. After the equilibrium was reached, the catalyst was recovered by filtration and re-used in a new reaction system fed with anhydrous methanol and the equilibrium was reached again.

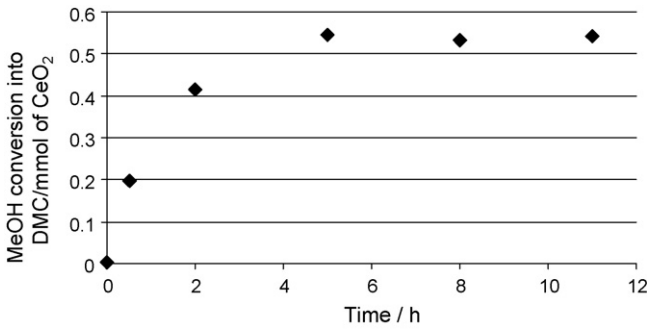

Fig. 2. Trend of the methanol conversion (mmol) into DMC with time per mmol of catalyst. In this test, 100 mg of CeO_2 were used with 4 mL of methanol at 408 K under 5.0 MPa of CO_2.

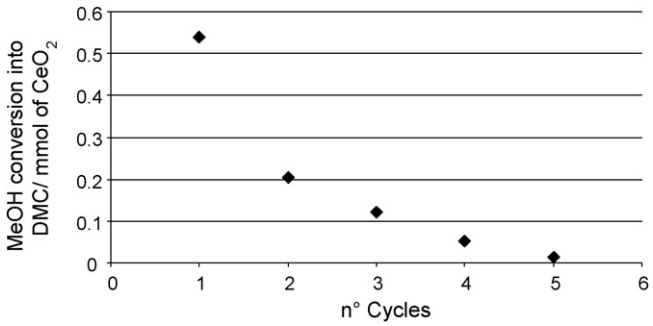

Fig. 3. DMC yield in five consecutive cycles of reactivity. In each cycle the same sample (100 mg) of CeO_2 was placed in a reactor with 4 mL of methanol, at 408 K for 3 h under 5.0 MPa of carbon dioxide.

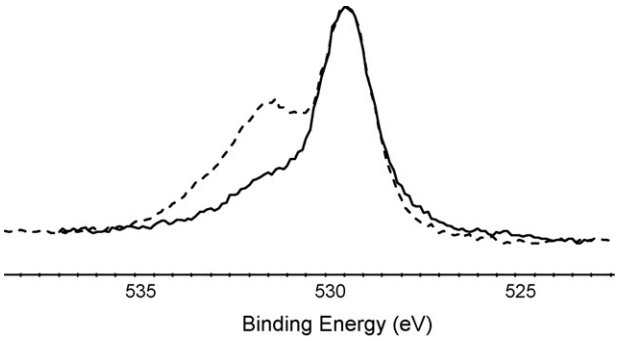

Fig. 5. XPS analysis on the oxygen atom region of commercial CeO_2 before (continuous line) and after (dashed line) one cycle.

This procedure was repeated several times. Fig. 3 shows that after the first cycle the activity of the catalyst steadily decreased to reach almost zero after five cycles.

Such de-activation can be due to several reasons. Although it was observed by other authors, a study addressed to identify the catalyst modification was never carried out. In order to shade light on the de-activation process, we have characterized the catalyst before and after each reaction cycle using XPS and XRD. The XPS analysis of the catalyst before and after the first catalytic run is shown in Fig. 4.

It is quite evident that during the operation in catalysis the surface of the catalyst undergoes transformation as demonstrated by the rising of the component due to Ce(III) that represents 18% of starting Ce(IV), as calculated from the peak intensity of the XPS spectrum according to the Shyu method [25]. Further information about the modification of the catalyst comes from the observation of the XPS-spectrum of the O-atom. Fig. 5 clearly shows a considerable modification of the absorption spectrum with the rise of the signal at 531.5 eV that is very weak in the starting material.

Such surface modification can be related to the reduced activity of ceria. XPS spectra show that such process continues and the catalyst change progresses with the number of cycles. An analysis of the catalyst has allowed to determine that the size of the particles (originally of the order of a few μm) increases during the utilisation. On the other hand, the cell parameters do not show any sensible change during the operations: in fact, in both spectra the peak positions for the equivalent Bragg angles are the same, as shown in Fig. 6.

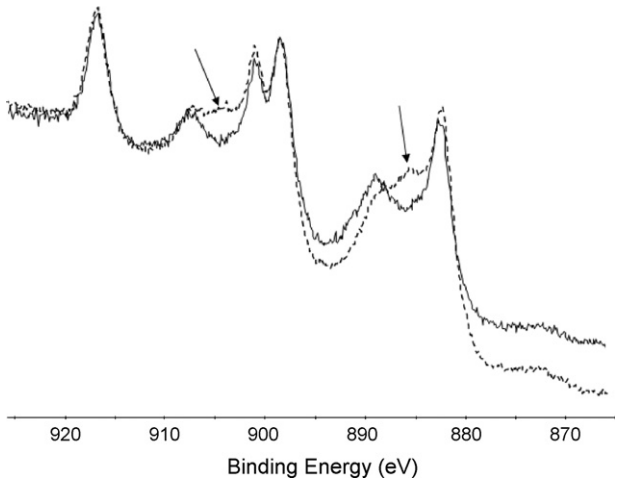

Fig. 4. XPS analysis of commercial CeO_2 on the cerium atom region before (continuous line) and after the first catalytic cycle (dashed line). The Ce(III) components are indicated with an arrow.

The reduction of Ce was coupled with the formation of the dimethylacetal of formaldehyde – $H_2C(OMe)_2$, found in the reaction solution at a concentration equivalent to the reduced fraction of Ce(IV). In order to understand whether the reduction of Ce(IV) to Ce(III) may cause the deactivation of the catalyst, we have used commercial Ce_2O_3 in the carboxylation of methanol and observed a very low activity (see Table 1, entry 4).

However, the XPS and XRD studies show that the catalyst particles undergo a minor structural change during the use, with a surface modification due to the partial reduction of Ce(IV) to Ce(III) and a change in the nature of the O-species. The broadening of the peaks at large values of 2θ may be due to such a minor distortion of the structure, which, noteworthy, is not restored with the heating. Interestingly, no $-O-CH_3$ moieties were observed (no reduced carbon signals observed by XPS), but only –OH-species were found. It is worth to emphasize that, as already noted by other authors [16b], the re-oxidation of the used catalyst does not produce a material with the same catalytic properties as the starting one. This may be due to the change in the reticular structure of the oxide, as reported above. The temperature plays a key role: higher temperatures produce less active catalysts.

3.2. New synthesis of CeO_2: its characterisation and utilisation in catalysis

In order to establish whether the activity of the catalyst depends on the preparation technique and on the size of particles, we synthesised CeO_2 according to the procedure reported in the Section 2. The XRD analysis of the ceria is shown in Fig. 7

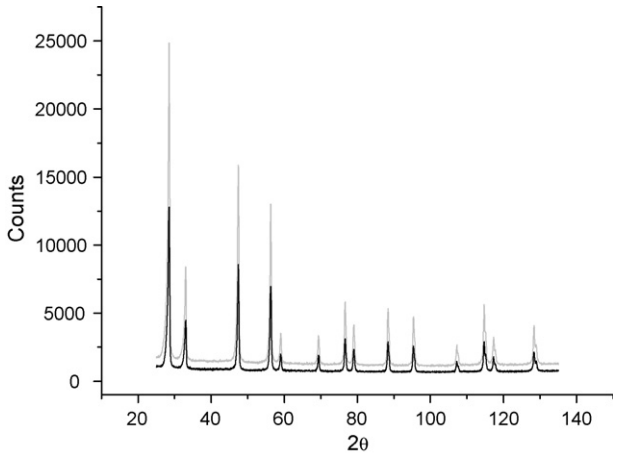

Fig. 6. XRD spectrum of commercial CeO_2 before (continuous black line) and after use in catalysis (dotted grey line).

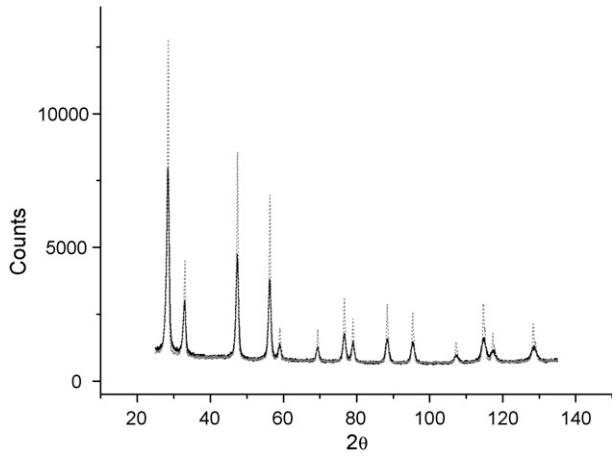

Fig. 7. XRD of CeO_2 synthesized (black line) compared with that of the commercially available sample (grey line).

(continuous black line) and compared with the spectrum of commercial ceria (grey line).

The FWHM is larger for the synthesised than for the commercial material, showing a lower crystallinity coupled to a smaller size of the particles which range around 5–20 nm. We used the synthesised CeO_2 in the carboxylation of methanol and controlled its behaviour by XPS and XRD.

The dotted line in Fig. 8 shows the XRD of the sample of synthesised CeO_2 after utilisation in catalysis: it is practically superimposable with that of the starting material, showing that no structural changes did occur. The XPS analysis of the surface of CeO_2 before and after utilisation in catalysis in the same conditions in which the commercial catalyst was used, shows that the catalyst synthesised in this work remains quite unchanged after use. The formation of Ce(III) is not quantifiable through the XPS spectrum. Consequently, dimethylacetal of formaldehyde is present in the reaction solution at trace level. Also, the BET area of the sample did not substantially change after use, as it remained in the range 60–75 $m^2\ g^{-1}$.

Fig. 9 shows that no reduction takes place and Fig. 10 demonstrates that the O1s high resolution spectrum is only marginally affected by use.

The newly synthesised CeO_2 catalyst when used in the carboxylation of methanol produced the results shown in

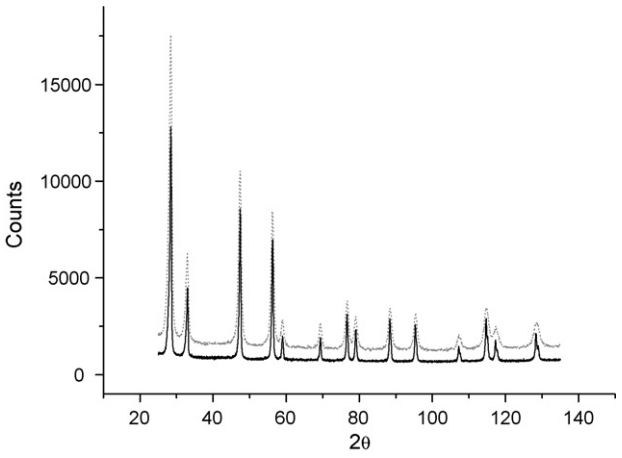

Fig. 8. XRD spectra recorded for synthesized-CeO_2 before (continuous) and after (dotted line) five cycles of catalysis.

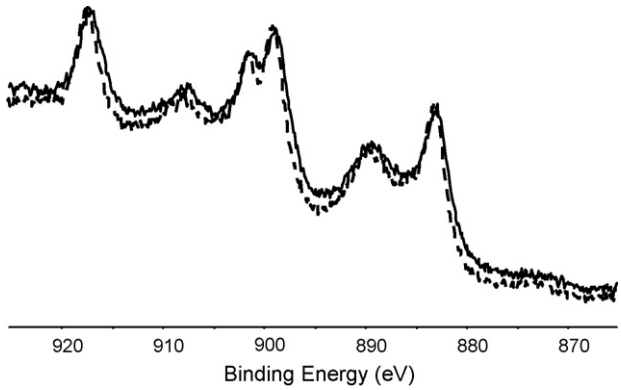

Fig. 9. XPS analysis of synthesized CeO_2 on the cerium atom before and after the first catalytic cycle.

Fig. 11 (◆ curve: compare with Fig. 3), it could be used in several cycles without any apparent deactivation.

It is worth to note the higher activity (0.6 mmol vs 0.54 mmol DMC/mmol catalyst after 3 h. The latter value has been calculated considering the total number of Ce-centres. In principle, only the Ce-centres present at the surface should be active. In order to be able to measure with higher accuracy the real activity of the catalyst we are now preparing samples in which the CeO_2 is supported on a surface so that the number of Ce-centres can be more accurately counted.) and stability. It can be inferred that the higher surface stability corresponds to a longer life and better activity: as a matter of fact, more than 30 mol of DMC were produced per each nominal Ce(IV)-oxide unit. These features seem to support the conclusion that there may be a connection between the surface modification and the deactivation of the catalyst that, on the other hand, not necessarily undergoes a substantial cell modification with use.

3.3. Catalyst modification: CeO_2 loaded with a second metal oxide

Following such discovery and knowing that mixed oxides may have a longer catalytic life than single metal oxides [26], we decided to prepare ceria catalysts loaded with another metal: we choose Al or Fe in our first attempts. Table 1 compares the activity of the single-metal or bi-metallic Ce-based catalysts, with that of other metals (entries 5–9).

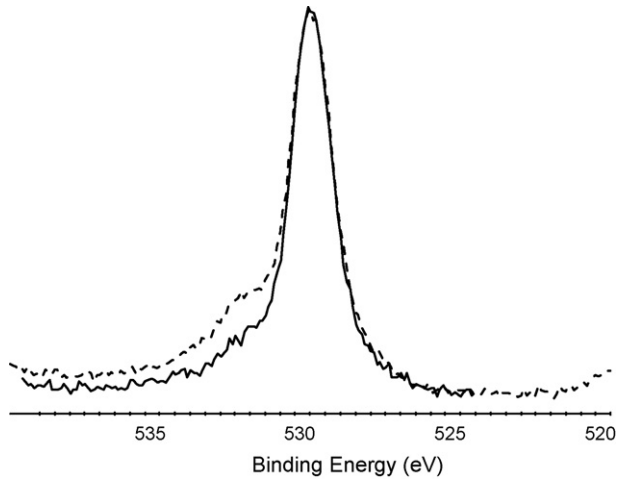

Fig. 10. XPS analysis of synthesized CeO_2 on the oxygen atom region before (black continuous line) and after (dotted line) the first catalytic cycle.

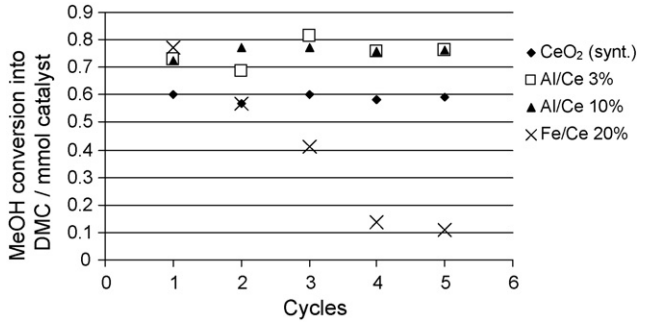

Fig. 11. Methanol conversion (mmol) into DMC for four different metal oxides. In each test, 4 mL of methanol and 100 mg of the oxide were placed in a stainless steel reactor under 5.0 MPa of carbon dioxide, at 408 K for 3 h.

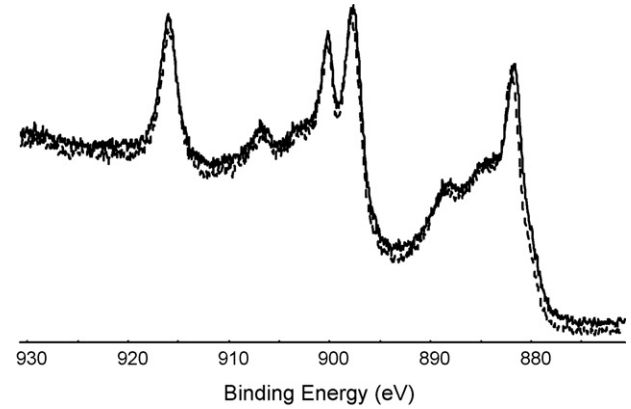

Fig. 12. XPS analysis of Al(10%)/Ce oxides on the cerium atom before and after the first catalytic cycle.

$Al(OH)_3$, $CeSO_4$, Ce_2O_3, La_2O_3, Fe_2O_3 and FeO alone were practically not active in the carboxylation of methanol. Conversely, CeO_2 loaded with Al at 3–10% was more active and more resistant than CeO_2 and it could be used for several days without any change of the activity (Fig. 11). Also Fe-loaded CeO_2 (Fig. 11) was quite interesting for its initial activity, but did not had a long life.

Fig. 12 shows that after the utilisation in catalysis the XPS spectrum of the Ce–Al sample in the Ce-zone remained unchanged, without any appearance of Ce(III). Also the O1s high resolution spectrum (Fig. 13) was not sensibly changed during catalysis.

Therefore, it seems that the presence of Al helps to avoid the surface modification. The XRD spectra (Fig. 14) demonstrate that there is no change of the peak profile and intensity after utilisation of the catalyst. This is a further confirmation of the stabilizing effect of Al on CeO_2.

Also in this case, Ce(IV) is not reduced to Ce(III) (dimethylacetal of formaldehyde can be hardly detected). In order to ascertain whether the content of Al may influence the behaviour of the catalyst we have prepared samples of CeO_2 with 3%, 10%, 20%, 40% of Al_2O_3. The X-ray powder diffraction technique has been used for getting structural information. The XRD spectra of CeO_2 alone and of CeO_2 with the different percentages of Al_2O_3, were compared. They do not exhibit remarkable differences. Only a slight peak enlargement and a modest peak displacement at large 2θ values, both more evident at 10% that at 3% Al_2O_3 loading, can be detected. The peak enlargement can be ascribed to the crystalline degree, which is reduced with the increase of the Al content. The peak displacement corresponds to small cell parameters variation. No further differences were evident. Moreover, no additional peaks were found so that all the patterns correspond to a single

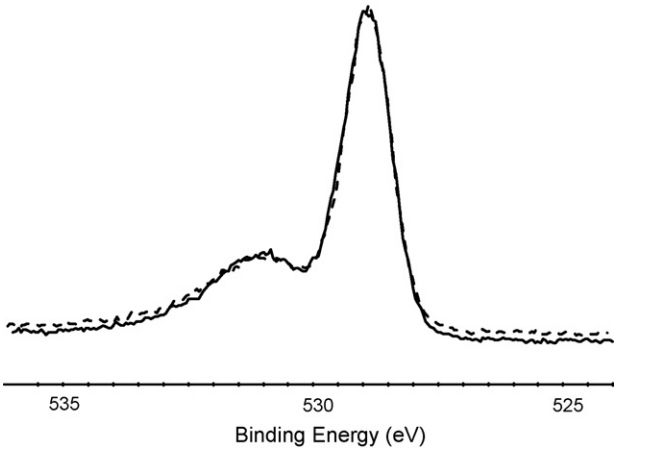

Fig. 13. XPS analysis of Al(10%)/Ce oxides on the oxygen atom before and after the first catalytic cycle.

crystalline phase, i.e. CeO_2. The crystal structure solution process shows only Ce and O site positions and does not reveal the Al location. In addition, being Al^{3+} smaller than Ce^{4+} (0.5 Å [27] against 1.04 Å [28]) it is likely that if Al had substituted Ce in the lattice position, a strong deformation of the cell would have been observed, with an unbalance of charges. In conclusion, the X-ray powder diffraction study does not reveal neither structural modifications nor an additional crystalline phase (Al_2O_3) besides the CeO_2. Additionally, at Al_2O_3 percentage above 10% a fine analysis of the background of the XRD-powders profile reveals the presence of an amorphous phase formed by alumina. On the basis of such data, we propose that at low Al-percentage (up to 10%), Al is randomly positioned in the CeO_2 cell, while above 10% loading an amorphous Al_2O_3-phase separates.

In order to get a confirmation to such picture, we have run the ^{27}Al CP-MAS NMR spectrum of the CeO_2-samples loaded with Al at different extents. Fig. 15 clearly shows that the 10% loaded CeO_2 exhibits a net signal at 40 ppm (attributed to "dispersed" alumina in the literature) [29] not found in Al_2O_3, while increasing the content of Al_2O_3 the signals of free Al_2O_3 peak-out besides the signal at 40 ppm. In particular the signal at 55 ppm can be attributed to a tetra-co-ordinated tetrahedral-Al and the signal at 7.4 ppm can be attributed to a six-co-ordinated octahedral-Al.

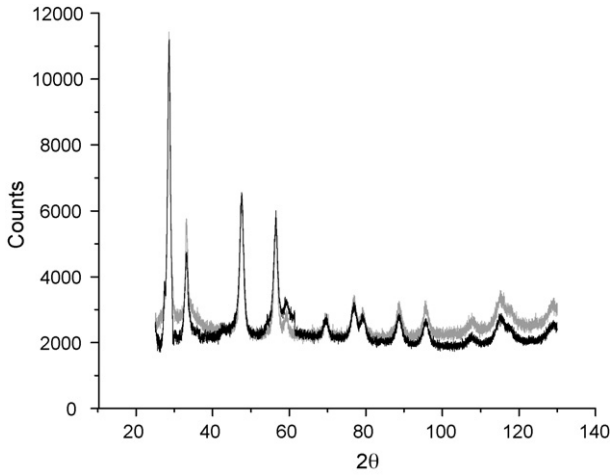

Fig. 14. XRD spectra recorded for Al/Ce oxides (10%) before (black) and after (grey line) five cycles of catalysis.

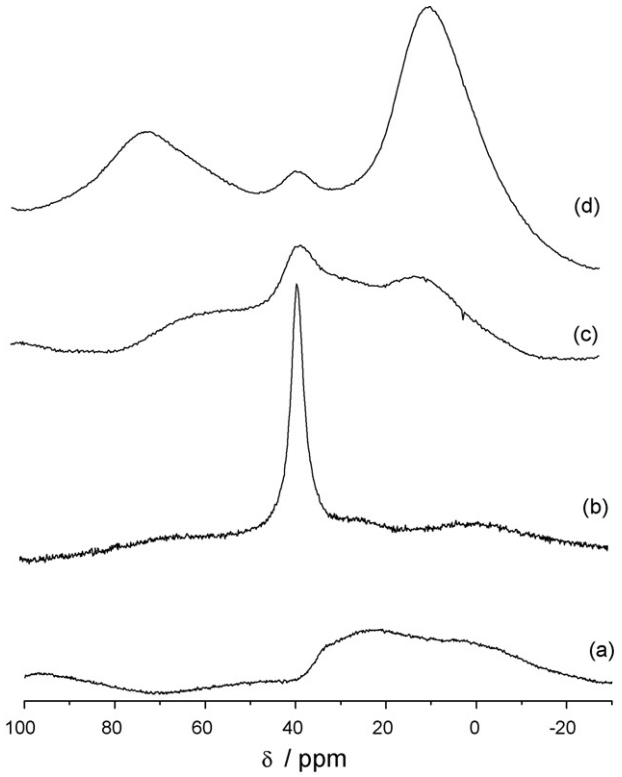

Fig. 15. MAS ^{27}Al NMR recorded on Al-Ce oxides at 3% (a), 10% (b), 20% (c) 40% (d) with a zirconia rotor at a speed of 5.0 kHz.

4. Conclusions

The data reported above seem to demonstrate that the de-activation of the commercial-CeO_2 catalyst is mainly due to a surface modification produced by the Ce(IV) to Ce(III) reduction during catalysis and to crystal conglomeration. In the ceria prepared in this work such effect is much reduced and is annulled in ceria loaded with 3–10% alumina. This causes a strong stabilization of the catalyst that can be used for several cycles without any de-activation and reaching an apparent TON of several tens. The lack of reduction of Ce(IV) to Ce(III) also reduces the change of the O1s high resolution spectrum of the XPS spectrum of ceria and this is also linked to a better activity of the catalyst. As foreseeable, the loading of a large amount of alumina in ceria does not produce a single phased more active catalyst, as alumina separates as an amorphous phase. The dimension of the particles is essential for an enhanced activity of the catalyst: nanoparticles with a 5–20 nm size seem to be the most active. The use of surface and structural techniques is very informative about the transformation that the catalyst undergoes with use. This is the first time that such a detailed analysis is carried out on a catalyst for alcohol carboxylation.

Following such discovery, we have undertaken a systematic study using several metals in order to ascertain the influence of the nature of the metal on the improvement of the life-time and efficiency of the CeO_2 catalyst.

Acknowledgements

The financial support by the EU-IP TOPCOMBI, MiUR and the University of Bari is gratefully acknowledged. The authors thank Giuseppe Chita of the Institute of Cristallography, CNR-Bari-Italy, for the technical assistance during XRD registration.

References

[1] (a) W.B. Kim, U.A. Joshi, J. Lee, Ind. Eng. Chem. Res. 43 (9) (2004) 1897;
(b) S. Fukuoka, M. Kawamura, K. Komiya, M. Tojo, H. Hachiya, K. Hasegawa, M. Aminaka, H. Okamoto, I. Fukawa, S. Konno, Green Chem. 5 (2003) 497.
[2] (a) D.-S. Tong, J. Yao, Y. Wang, H.-Y. Niu, G.-Y. Wang, J. Mol. Catal. A: Chem. 268 (1–2) (2007) 120;
(b) T. Chen, H. Han, J. Yao, G. Wang, Catal. Comm. 8 (9) (2007) 1361;
(c) Z. Du, W. Kang, T. Cheng, J. Yao, G. Wang, J. Mol. Catal.: Chem. 246 (1–2) (2006) 200;
(d) F. Mei, Z. Pei, G. Li, Org. Process Res. Dev. 8 (3) (2004) 372;
(e) S.R. Kirumakki, N. Nagaraju, K.V.R. Chary, S. Narayanan, Appl. Catal. A: Gen. 248 (1–2) (2003) 161.
[3] (a) A.B. Shivarkar, S.P. Gupte, R.V. Chaudhari, J. Mol. Catal. A: Chem. 226 (1) (2005) 49;
(b) S.R. Kirumakki, N. Nagaraju, K.V.R. Chary, S. Narayanan, J. Catal. 221 (2) (2004) 549;
(c) N. Nagaraju, G. Kuriakose, New J. Chem. 27 (4) (2003) 765;
(d) M.B. Talawar, T.M. Jyothi, T. Raja, B.S. Rao, P.D. Sawant, Green Chem. 2 (6) (2000) 266;
(e) K. Sreekumar, T. Mathew, S.P. Mirajkar, S. Sugunan, B.S. Rao, Appl. Catal. A: Gen. 201 (1) (2000) L1;
(f) T. Beutel, J. Chem. Soc. Far. Trans. 94 (7) (1998) 985.
[4] M. Distaso, E. Quaranta, Tetrahedron 60 (2004) 1531.
[5] G. Kuriakose, J.B. Nagy, N. Nagaraju, Catal. Comm. 6 (1) (2005) 29.
[6] (a) R. Luque, J.M. Campelo, T.D. Conesa, D. Luna, J.M. Marinas, A.A. Romero, New J. Chem. 30 (8) (2006) 1228;
(b) G. Vasapollo, G. Mele, A. Maffei, R. Del Sole, Appl. Organomet. Chem. 17 (11) (2003) 835;
(c) X. Jiang, A. Tiwari, M. Thompson, Z. Chen, T.P. Cleary, T.B.K. Lee, Org. Process Res. Dev. 5 (6) (2001) 604;
(d) S.R. Kirumakki, N. Nagaraju, K.V.V.S.B.S.R. Murthy, S. Narayanan, Appl. Catal. A: Gen. 226 (1–2) (2002) 175.
[7] V. Serini, in Ullmann's Encyclopedia of Industrial Chemistry, vol. A5, Weinheim, VCH Publishers, 1992, p. 197.
[8] (a) U. Romano, R. Tesei, M.M. Massi, P. Rebora, Ind. Eng. Chem. Prod. Res. Dev. 19 (3) (1980) 396;
(b) U. Romano, Chim. Ind. (Milan) 75 (4) (1993) 303;
(c) K. Nishihira, S. Tanaka, K. Kodama, T. Kaneko, Eur. Pat. Appl. EP. 501 (1992) 507.
[9] (a) D. Ballivet-Tkatchenko, S. Chambrey, R. Keiski, R. Ligabue, L. Plasseraud, P. Richard, H. Turunen, Catal. Today 115 (1–4) (2006) 80;
(b) D. Ballivet-Tkatchenko, O. Douteau, S. Stutzmann, Organometallics 19 (2000) 4563.
[10] (a) M. Aresta, A. Dibenedetto, C. Pastore, Inorg. Chem. 42 (10) (2003) 3256;
(b) M. Aresta, A. Dibenedetto, C. Pastore, Catal. Today 115 (2006) 88.
[11] T. Sakakura, J.-C. Choi, H. Yasuda, Chem. Rev. 107 (2007) 2365;
T. Sakakura, Y. Saito, J.-C. Choi, T. Sako, Polyhedron 19 (2000) 573.
[12] T. Sakakura, Y. Saito, J.-C. Choi, T. Masuda, T. Sako, T. Oriyama, J. Org. Chem. 64 (1999) 4506.
[13] T. Sakakura, Y. Saito, M. Okano, J.-C. Choi, T. Sako, J. Org. Chem. 63 (1998) 7095.
[14] J.-C. Choi, L.-N. He, H. Yasuda, T. Sakakura, Green Chem. 4 (2002) 230.
[15] M. Aresta, A. Dibenedetto, E. Fracchiolla, P. Giannoccaro, C. Pastore, I. Pápai, G. Shubert, J. Org. Chem. 70 (16) (2005) 6177.
[16] (a) K. Tomishige, Y. Furusawa, Y. Ikeda, M. Asadullah, K. Fujimoto, Catal. Lett. 76 (2001) 71;
(b) K. Tomishige, Y. Yoshida, Y. Arai, S. Kado, K. Kunimori, Catal. Today 115 (2006) 95.
[17] (a) K. Tomishige, T. Sakaihori, Y. Ikeda, K. Fujimoto, Catal. Lett. 58 (1999) 225;
(b) K. Tomishige, T. Sakaihori, Y. Ikeda, K. Fujimoto, J. Catal. 192 (2000) 355.
[18] S.-H. Zhong, L.-L. Kong, H.-S. Li, X.-F. Xiao, Ranliao Huaxue Xuebao 30 (5) (2002) 454.
[19] D.D. Perrin, W.L.F. Armarego, D.R. Perrin, Purification of Laboratory Chemicals, Pergamon Press, Oxford, England, 1986.
[20] Bruker AXS; DIFFRAC^{plus} EVA, EVA Application, Version 8, 0, 0, 2. Bruker AXS. Karlsruhe, Germany.
[21] A. Altomare, M.C. Burla, M. Camalli, B. Carrozzini, G. Cascarano, C. Giacovazzo, A. Guagliardi, A.G.G. Moliterni, G. Polidori, R. Rizzi, J. Appl. Cryst. 32 (1999) 339.
[22] J. Rodríguez-Carvajal, Phys. B 192 (1993) 55.
[23] Bruker AXS; TOPAS, Version 2.0. Bruker AXS. Karlsruhe, Germany.
[24] R.A. Young, The Rietveld Method, IUCR Monographs on Crystallography 5, Oxford University Press, Oxford, 1993.
[25] J.Z. Shyu, W.E. Weber, H.S. Gandhi, J. Phys. Chem. 92 (17) (1988) 4964.
[26] D. Terribile, A. Trovarelli, C. de Leitenburg, A. Primavera, G. Dolcetti, Catal. Today 47 (1999) 133.
[27] L. Pauling, The Nature of the Chemical Bond, 3d ed., Cornel University Press, Ithaca, N.Y., 1960.
[28] R.D. Shannon, Acta Crystallogr. A32 (1976) 751.
[29] R. Sasikala, V. Sudarsan, S.K. Kulshreshtha, J. Solid State Chem. 169 (2002) 113.